Air Distribution in Rooms, (ROOMVENT 2000)
Editor: H.B. Awbi

EXPERIMENTAL INVESTIGATION OF THE VELOCITY FIELD AND AIR FLOW PATTERN GENERATED BY COOLING CEILING BEAMS

Jan Fredriksson*,†, Mats Sandberg† and B. Moshfegh*

* Division of Energy and Production Systems
University of Gävle
S-801 76 Gävle, Sweden

† Department of Built Environment
Royal Institute of Technology
S-801 02 Gävle, Sweden

ABSTRACT

In the modern office environment there are numerous heat generating equipment. In addition there are loads from solar radiation and heat produced by people. Therefore, the loads will often exceed the load the ventilation system can cope with. To meet this demand on extra cooling capacity the commercial market provides cooling ceiling panels and cooling beams. A literature review shows that until now the majority of the research has been focused on the cooling performance and only a minor part on the thermal comfort and air quality.

A cooling beam is a source of natural convection, creating a transport of cold air into the occupied zone. Furthermore, natural convection flows are vulnerable to disturbances.

Experiments have been conducted in a mock up of an office room. A large variety of heating loads have been used. Qualitative information has been obtained by the use of visualisation, registered by a digital video camera. The time history of velocity and temperature has been registered. The change in position (oscillations) with time of the air-flow generated by the chilled beam has been documented by the use of small and fast thermo-couples and thermistor anemometers.

The results show that the air-flow from the chilled beam exhibits strong oscillations both sideways and along the chilled beam. Furthermore, air-flow generated by heat sources in the room may reverse the flow generated by the chilled beam.

KEYWORDS

Cooling ceiling beams, Measurements, Natural Convection, Plume flow.

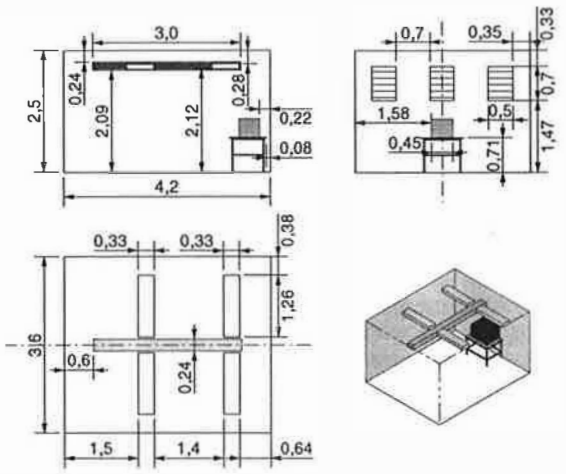

Figure 1. Room layout. All measures in meter.

EXPERIMENTAL SET UP, ROOM LAYOUT

A test room (L x W x H, 4.2 m x 3.6 m x 2.5 m) was set-up to provide a realistic office environment, see figure 1.

To mimic a common office environment the room was furnished with a PC-model with variable heat generation and a "mannequin" with approximately the same area and heat load as a human. In the test room a chilled beam (L_B x W_B x H_B, 3.0 m x 0.24 m x 0.17 m) was installed 0.24 m below the ceiling. The inlet water to the chilled beam was held at a nearly constant temperature of 14.7 °C and the water flow-rate was kept constant at $3{,}6 \times 10^{-5}$ m^3/s. Electric heating foil was used to simulate solar irradiated windows and the lighting was provided by four fluorescent tube fittings. For the quantitative measurements the following three heat-sources were used; fluorescent tube fittings (347 W), PC-model (443 W) and electric heating-foil (345 W).

The heat-loads were combined into three cases as shown in table 1 together with the corresponding cooling power of the chilled beam. The differences between heat-load and cooling power is due to heat transmission through the room walls.

Case	*Heat-sources*	*Heat-load [W]*	*Beam Cooling Power [W]*
A	Fluorescent tube fittings	347	301
B	Fluorescent tube fittings, PC-model	790	609
C	Fluorescent tube fittings, PC-model, heating foil (window)	1135	777

Table 1. Heat balance for the three test cases.

The room surface- and air-temperature were measured with a large number of thermo-couples. The cooling power of the chilled beam was assessed by measuring the temperature difference between inlet and outlet together with the flow-rate.

FLOW PATTERN MEASUREMENTS

The qualitative properties of the global characteristics of the flow pattern were obtained by visualisation by smoke together with laser light or white light illumination. This was documented with the use of a digital camera or a video recorder.

To quantitatively examine the velocities and fluctuations a 26-channel thermistor anemometer system were used. The anemometer system, CTA88, is specially designed for the typically low velocities in room flow, see Lundström et. al. (1990). The data were acquired with a sampling frequency of 2 Hz. The numbers of samples for all cases were 10240 giving a total measuring time of 5120 seconds. The probes were calibrated in downward flow and fitted with a least-square relation according to the well-known Siddal-Davies correlation. The probes were all mounted in a row attached on a tube and the probe spacing was selected in relation to the actual plume width. Traversing of the probes were made with a computer-controlled traversing system. Measurements were carried in downstream direction to a distance where the plume was beginning to dissolve and no further reliable measurements could be made.

THEORY

The air-flow generated by the chilled beam is treated as a negatively buoyant plume. The following reasoning can be found in Sandberg and Etheridge (1996).

The driving force for the air-flow generated by the chilled beam is caused by the buoyancy forces occurring due to temperature differences between the chilled beam and the surrounding air. The theoretical velocity for a two-dimensional line source can be expressed as a function of the specific convective buoyancy flux at the source, *B(0)*. After an initial developing phase, assuming a normal distribution of velocity and temperature distribution, the following expression is obtained,

$$u(c) = 2.45B(0)^{1/3} \qquad (1)$$

where

$$B(0) = \frac{g\beta q}{\rho c_p} \qquad (2)$$

and

$u(c)$ = *centre-velocity of the plume [m/s]*
g = *acceleration by gravity [m/s^2]*
β = *volume coefficient of expansion [K^{-1}]*
q = *convective heat transfer rate per meter [W/m]*
ρ = *density [kg/m^3]*
c_p = *specific heat at constant pressure [J/kg·K]*

In the analysis of plumes in the atmosphere has Scorer (1978) presented a relation for the acceleration of a buoyancy-driven plume with non-negligible area source. This relation indicates that the width diminution within the nonentrainment zone is varying with distance from the source, i.e.:

$$W \propto z^{-1/2} \qquad (3)$$

where

W = *width of the plume [m]*
z = *distance from source [m]*

RESULTS

GLOBAL CHARACTERISTICS

The results indicate that the flow through the chilled beam is rather unstable. Figure 2 shows a sequence from the video recording. Smoke has been introduced into the beam. Close to the beam there

Figure 2. Laser light visualisation from Case B, 25 seconds between each frame.

is a slow drift across the width of the beam. At the beginning the flow is laminar (white continuos sheet) and exhibits a meandering motion until the point where there is a transition to turbulent motion with associated vortex motions and entrainment of ambient air. The dark areas within the plume are interpreted as consisting of entrained ambient air. The point of transition oscillates occurs within an interval equal to 1 W_B -2 W_B.

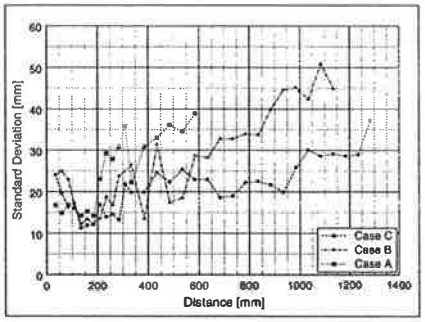

Figure 3. Standard deviation of change in position below the beam.

These oscillations become stronger when the cooling power is reduced and less pronounced at higher heat-loads. The chart in figure 3 shows the standard deviation of the change of position. It can be seen that the standard deviation decreases from case **A** to case C. Similar oscillation phenomenon can also be observed along the beam. The air-flow is not uniformly generated along the beam. The air flow-rate is sometimes higher through one end of the chilled beam than through the other.

The interaction with other heat-sources is strong. Heat-sources located near the boundary of the plume or within the plume will influence the plume strongly. It is e.g. very easy to turn the flow from downwards to upwards by placing a heat-source below the beam. Furthermore, the plume gets attracted towards warmer surfaces and the air-flow will thereafter turn upward along the surfaces.

LOCAL CHARACTERISTICS

If the maximum velocity is interpreted as the centre of the downward plume, the results from the velocity measurements verifies the observation from above. There are fluctuations in the direction of the plume centre-line, however, the fluctuations are of rather slow nature. Examples from the cross-wise velocity-measurements are shown in figure 4. There are also shown the fluctuations in the mean velocity. It can be noted that the velocity fluctuations, compared to the other examples, are of largest magnitude at a distance of 235 mm from the beam.

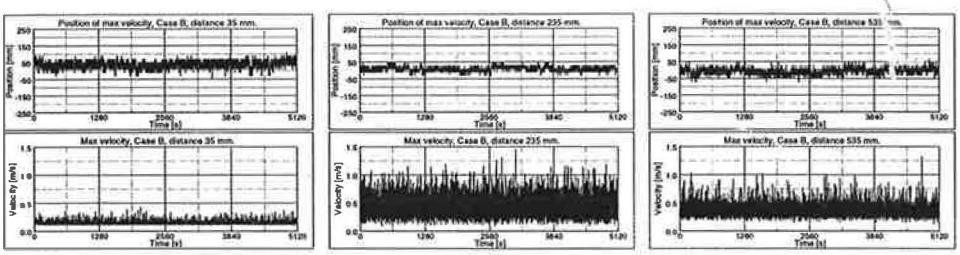

Figure 4. Change in position and maximum velocity fluctuations, Case B at distances of 35 mm (left), 235 mm (middle) and 535 mm (right) from the chilled beam.

The width of the plume is defined as the distance from the position of the local mean maximum velocity to the point, where the velocity has decreased to half the value of the local mean maximum velocity. It can bee seen in figure 5 that there is an acceleration phase very close to the chilled beam. The width decreases and the plume becomes thinner in the near region of the beam. After a certain distance the width starts to grow linearly. In the same region the velocity at first increases to obtain a maximum value and thereafter it exhibits a slow decay.

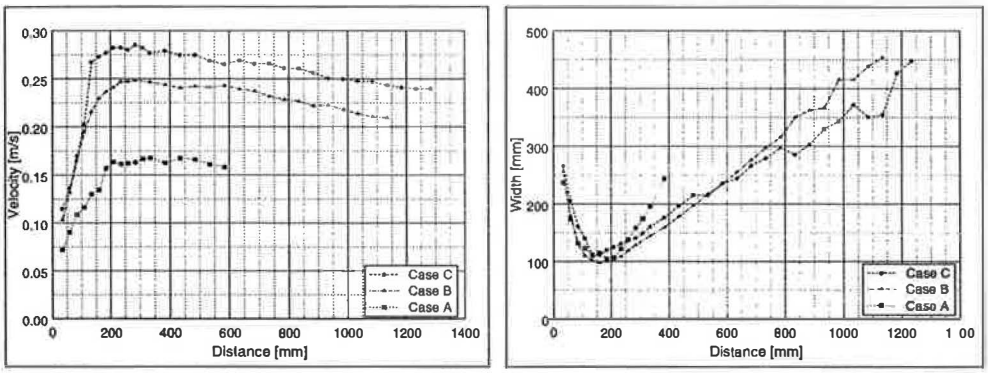

Figure 5. Mean maximum local velocity (left) and plume width (right).

As discussed in previous paragraph, the plume is attracted by nearby surfaces with higher temperature than the plume. This phenomenon is observed in all three test cases when the plume gets attracted to the walls of the room. In figure 6 the profiles of the plumes are shown. In case B and C the plume is deviated to the left-hand side but, in case A, the plume bends to the opposite side. This is the result of different boundary condition at the walls, in case B and C the left wall is warmer than the right and in case A it is the opposite.

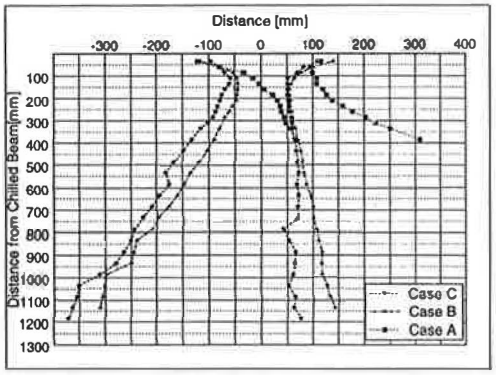

Figure 6. Profiles of the plumes.

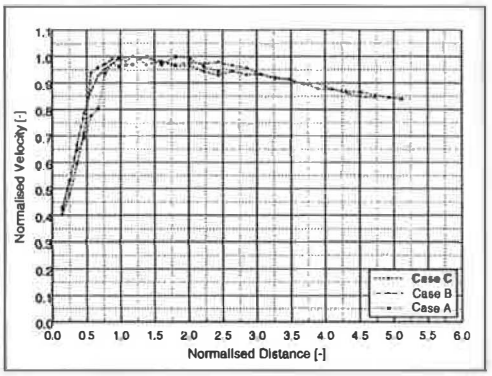

Figure 7. Normalised local mean velocity.

DISCUSSION AND CONCLUSION

Figure 7 shows the normalised local maximum mean velocity as a function of the normalised distance from the chilled beam. The normalised local maximum mean velocity is the ratio of local maximum mean velocity and the maximum velocity at the corresponding test case, the normalised distance is the ratio of the distance from the beam and the beam with, W_b.

The graphs from the different test cases coincide quite well. This indicates that neither the acceleration phase nor downstream decelerations, with a possible exception for Case A, are particularly dependent of the cooling load. The dependency is in the magnitude of the velocity. As noted in formula (1), the theoretical centre-velocity should become constant and proportional to the convective specific buoyancy per meter raised to one-third. The heat transfer in this case is in fact both convection and radiation.

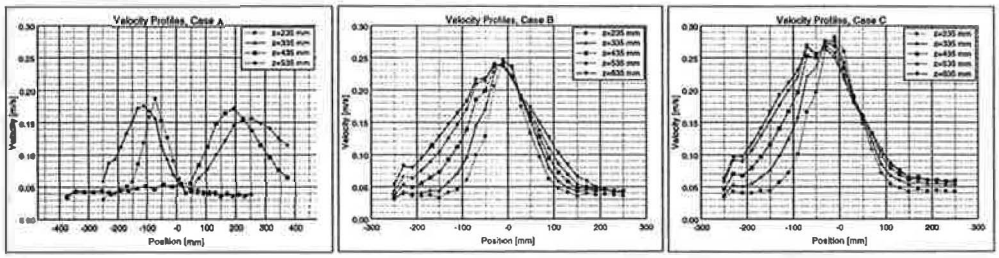

Figure 8. Velocity-profiles at different location from the chilled beam.

In figure 8 are the velocity-profiles from the three case shown at different distances from the beam. It is notable that the measurements indicate velocities next to the beam. Therefore an additional reasonable reduction factor is the underlying circulation of air that the beam generates in the room. This theory is summarised in table 2 with the assumptions; the convection heat transfer is reduced with 50% due to radiation and the background velocity is deducted with estimations from figure 8. The slow decay in velocity can probably be attributed to that the plume is not an ideal two-dimensional plume because it is generated by a cooling beam of finite length.

Case	*Convective Specific Buoyancy Flux, B(0) [m^3/s^3]*	*Theoretical Velocity [m/s]*	*Background velocity reduction [m/s]*	*Resulting velocity [m/s]*	*Measured Velocity [m/s]*
A	0.00136	0.271	0.035	0.235	0.16
B	0.00275	0.343	0.040	0.303	0.24
C	0.00351	0.372	0.050	0.322	0.28

Table 2. Assessment of velocities assuming 50% convective heat transfer.

Interesting observation can be made by comparing the actual distribution of the location of the local maximum velocity and the Gaussian normal distribution. This is shown in figure 11 for three examples from case B, at different locations from the beam. It can be seen that the actual distribution can be interpreted as normal distributed. The discrepancies are caused by insufficient spatial resolution.

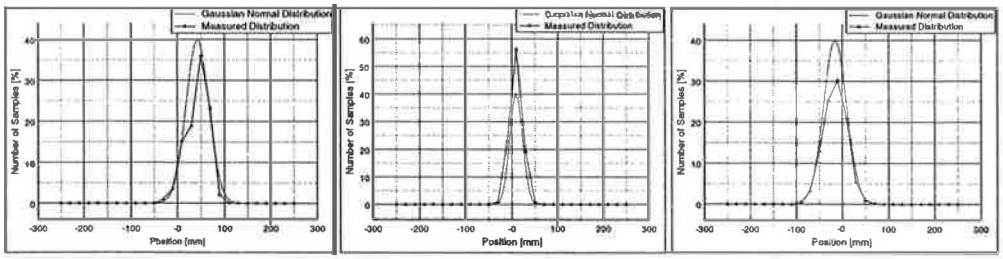

Figure 9. Gaussian normal distribution of change in position at different location from the chilled beam.

To conclude this paper it can be said that the air-flow generated by a chilled beam involves strong (two-dimensional fluctuations) of a rather slow nature. The fluctuations are dependent on the cooling power produced by the chilled beam, as the stability of the plume will increase with increasing cooling power. The spreading of the plume is sensitive to the presence of other heat-sources. The plume is attracted towards surfaces with higher temperature and a heat-source placed underneath the beam can reverse the plume flow generated by the plume.

ACKNOWLEDGEMENT

The help from Mr. Claes Blomqvist, Mr. Hans Lundström and Mr. Ragnvald Pelltari in various shapes of the project is gratefully acknowledged.
This project is sponsored by KK Foundation, Stockholm Sweden, and University of Gävle, Gävle Sweden.

REFERENCES

Hans Lundström, Claes Blomqvist, Perolof Jonsson and Ingemar Pettersson. (1990)
A Microprocessor-Based Anemometer for Low Air Velocities,
Proceedings of Roomvent 1990, Session B1:27

Etheridge, David W. and Sandberg, Mats. (1996)
Building Ventilation: Theory and measurement. Wiley, Chichester

Scorer, Richard Segar. (1978). *Environmental Aerodynamics*
Halsted, New York